ISSN 1573-160X, *PHYSICAL OCEANOGRAPHY*, Vol. 30, Iss. 5, pp. 563-580 (2023)

published in *Morskoy Gidrofizicheskiy Zhurnal*, 2023, Vol. 39, Iss. 5, pp. 599–616.

Original article

Average Climatic Characteristics of Internal Waves in the Sea of Japan Based on the WOA18 Atlas

M. V. Kokoulina [1, 2], O. E. Kurkina [1], T. G. Talipova [2, 3], A. A. Kurkin [1, 2, ✉], E. N. Pelinovsky [2, 3, 4]

[1] *Nizhny Novgorod State Technical University n.a. R. E. Alekseev, Nizhny Novgorod, Russian Federation*
[2] *V. I. Il'ichev Pacific Oceanological Institute, Far Eastern Branch of Russian Academy of Sciences, Vladivostok, Russian Federation*
[3] *A. V. Gaponov- Grekhov Institute of Applied Physics, Russian Academy of Sciences, Nizhny Novgorod, Russian Federation*
[4] *HSE University, Moscow, Russian Federation*
✉ *aakurkin@gmail.com*

Abstract
Purpose. The study is aimed at constructing the atlas, or a set of charts, for kinematic and nonlinear parameters of internal waves of the lowest mode in the Sea of Japan for mapping the region according to possible wave forms, and for determining polarities (elevation or depression) and limiting amplitudes of solitary internal waves.
Methods and Results. Based on hydrological data for the long-term average seasons derived from the climatological atlas WOA18, the seasonal features of density stratification of the Sea of Japan waters and the related kinematic and nonlinear parameters of internal waves governed by the environment are considered. For this purpose, the numerical solutions of a linear boundary value problem for internal waves are constructed that results in determining the wave phase velocities and the vertical structure (mode) of the wave fields for each calculation point. This basis allows numerical construction of the remaining characteristics, namely, the dispersion parameter, the quadratic and cubic nonlinearity parameters which make it possible to classify the localized non-radiating internal waves.
Conclusions. The atlas is intended both for express assessing the internal wave characteristics, forecasting possible scenarios of their generation and transformation, and for more detailed modelling of their propagation. The estimates obtained can also be used to analyse the effect of internal waves on the propagation of acoustic signals in the water column, the redistribution of suspended particles including nutrients and living organisms, and the transport of bottom sediments.

Keywords: density stratification, internal waves, Sea of Japan

Acknowledgements: The work was supported by the Laboratory of Nonlinear Hydrophysics and Natural Disasters of the V. I. Il'ichev Pacific Oceanological Institute, FEB of RAS, grant of the Ministry of Science and Higher Education of Russian Federation (agreement No. 075-15-2022-1127 dated July 1, 2022).

For citation: Kokoulina, M.V., Kurkina, O.E., Talipova, T.G., Kurkin, A.A. and Pelinovsky, E.N., 2023. Average Climatic Characteristics of Internal Waves in the Sea of Japan Based on the WOA18 Atlas. *Physical Oceanography*, 30(5), pp. 563-580.

Introduction

Internal waves, which exist due to the density differentiation of water layers, are responsible for many processes occurring in the ocean. These include mixing of ocean waters, transport of dissolved substances and suspended particles, and influence on surface waves. Internal waves play an important role in the functioning of ecosystems, in particular planktonic ones [1]. They are

considered to be responsible for the erosion of the sea platform bases and for the death of submarines, they also greatly distort acoustic signals propagating in the sea [2–5]. The most dangerous for underwater vehicles and structures are internal waves of large amplitude, which often have soliton-like shapes of different polarities and different modes, mainly the first and second mode [1] [6–8]. Sometimes, a steep front of an internal wave breaks up into a chain of solitons (solibors), which are often found on a shelf, for example, in the Sea of Japan [9]. In stratified ocean waters, quite compact packets of internal waves are also found, shaped like breathers well known in physics [7, 10].

When studying internal waves, the stratification of the waters in the water area, both density and shear flow, is first considered. To estimate the influence of stratification on the parameters of internal waves in the sea, well-known data arrays with averaged hydrological fields are usually used. Isolating such characteristics as the value of the maximum Brunt-Väisälä frequency, as well as this maximum depth, can benefit from a deeper understanding of the internal wave behaviour during their propagation. Maps of the Brunt-Väisälä frequency maximum values and maps of its depth for the Baltic, Mediterranean, South China seas, and the Sea of Okhotsk, constructed by the authors earlier, are given in [11–14]. In the Sea of Japan, as in all the seas of the Pacific Ocean, the main reason for the internal wave generation is the barotropic tide, although internal waves also propagate in non-tidal seas such as the Mediterranean, Black, Baltic, and Caspian, in fairly large lakes and water bodies [15, 16].

The most dangerous and interesting are internal waves of moderate and large amplitudes (20–100 or more meters in isopycnal displacement), being mainly nonlinear in nature. Their frequent occurrence in shelf zones confirms the need to study them once again. The above-mentioned identifiable forms of nonlinear internal waves and their evolution in a stratified ocean are well described by stationary solutions of the Gardner equation [17], obtained from the Euler equations for vertically stratified fluid in the approximation of weakly nonlinear and weakly dispersive waves. The internal wave dynamics model built based on the Gardner equation allows, based on its parameters, expressing estimation of the stationary wave types, describing their evolution and possible amplitudes.

The present paper is devoted to the description of the geographical features of the density stratification of the Sea of Japan, its seasonal variability as a background for the development of processes associated with internal waves, as well as maps of the kinematic parameters of internal waves constructed based on mean climatic hydrological data.

As initial data for constructing maps of internal wave parameters within the Gardner equation framework for horizontally inhomogeneous environment, the open-source digital climatological atlas *World Ocean Atlas 2018* (WOA18) was used. It integrates generalized and standardized information about the main features of hydrophysical parameters of sea water and their seasonal changes. It contains arrays of averaged and smoothed data from field measurements of temperature,

[1] Apel, J.R., Ostrovsky, L.A., Stepanyants, Y.A. and Lynch, J.F., 2006. *Internal Solitons in the Ocean*. Technical Report. WHOI-2006-04. Woods Hole: Woods Hole Oceanographic Institution, 110 p.

salinity, and other hydrological parameters [2]. WOA18 data are used on a regular grid with a resolution of 5°, 1° or 1/4° and represent vertical profiles of temperature and salinity averaged over a mean climatic year, season, and month at 137 vertical levels. We used salinity and temperature data for the summer and winter periods, based on which, using the TEOS10 seawater equation of state (http://teos-10.org/), its potential density was restored and the Brunt-Väisälä frequency was calculated.

Stratification of the Sea of Japan waters

The Sea of Japan is a semi-enclosed marginal sea of the Pacific Ocean, one of the largest and deepest seas in the world. One of the features of the generally warm Sea of Japan is the cold water inflow through the Tatar Strait in May – June due to the ice melting in the cold Sea of Okhotsk. Therefore, the stratifications of the northern and southern parts of the Sea of Japan should be very different from each other, especially in summer. A map of the Sea of Japan region with fairly detailed bathymetry is shown in Fig. 1.

The present paper contains maps of the density stratification features of the Sea of Japan waters, calculated from averaged data for summer and winter periods to show the maximum difference in stratification. These and other maps were compiled using *Ocean Data View* software [3] . The maps and histograms produced are based on the WOA18 atlas [2] reference points.

To analyze the density stratification of sea water from the view point of its influence on the field parameters of possible internal gravity waves, maps of the maximum values of the Brunt-Väisälä frequency (buoyancy frequency) N_{max} and maps of this value maximum depth throughout the Sea of Japan for winter and summer seasons were constructed. These maps demonstrate (Figs. 2, 3) that the density stratification of the Sea of Japan depends on the season significantly. Thus, in summer there is a noticeable increase (up to 4 times) in N_{max} values compared to winter, along with a simultaneous decrease in the pycnocline depth, when the Brunt-Väisälä frequency maximum tends to a value of 0.04 s^{-1}. This rather large maximum is characteristic of almost the entire central and southwestern waters of the Sea of Japan. In winter, it drops to 0.01 s^{-1} almost throughout the entire sea area, only rising slightly to 0.017 s^{-1} near the Honshu Island coast. Accordingly, histograms constructed for N_{max} show a wide spread in summer (0.017–0.04 s^{-1} with a most probable value of 0.032 s^{-1}) and a narrow distribution in winter (0.002–0.02 s^{-1} with the most probable value of 0.07 s^{-1}). It should be noted that in winter the highest values of the maximum buoyancy frequency are grouped in the southeast of the sea, near the Honshu Island coast and practically in the coastal zone of Peter the Great Bay, as well as near Cape Schultz. In summer, they are smaller near the Honshu Island coast than on the southwestern coast of the sea.

---

[2] Garcia, H.E., Boyer, T.P., Baranova, O.K., Locarnini, R.A., Mishonov, A.V., Grodsky, A., Paver, C.R., Weathers, K.W., Smolyar, I.V. [et al.], 2018. *World Ocean Atlas 2018: Product Documentation*. Silver Spring, MD: Ocean Climate Laboratory NCEI/NESDIS/NOAA, 20 p. Available at: https://www.ncei.noaa.gov/archive/accession/NCEI-WOA18 [Accessed: 21 May 2023].

[3] Alfred Wegener Institute. 2023. *Ocean Data View*. [online] Available at: https://odv.awi.de [Accessed: 04 October 2023].

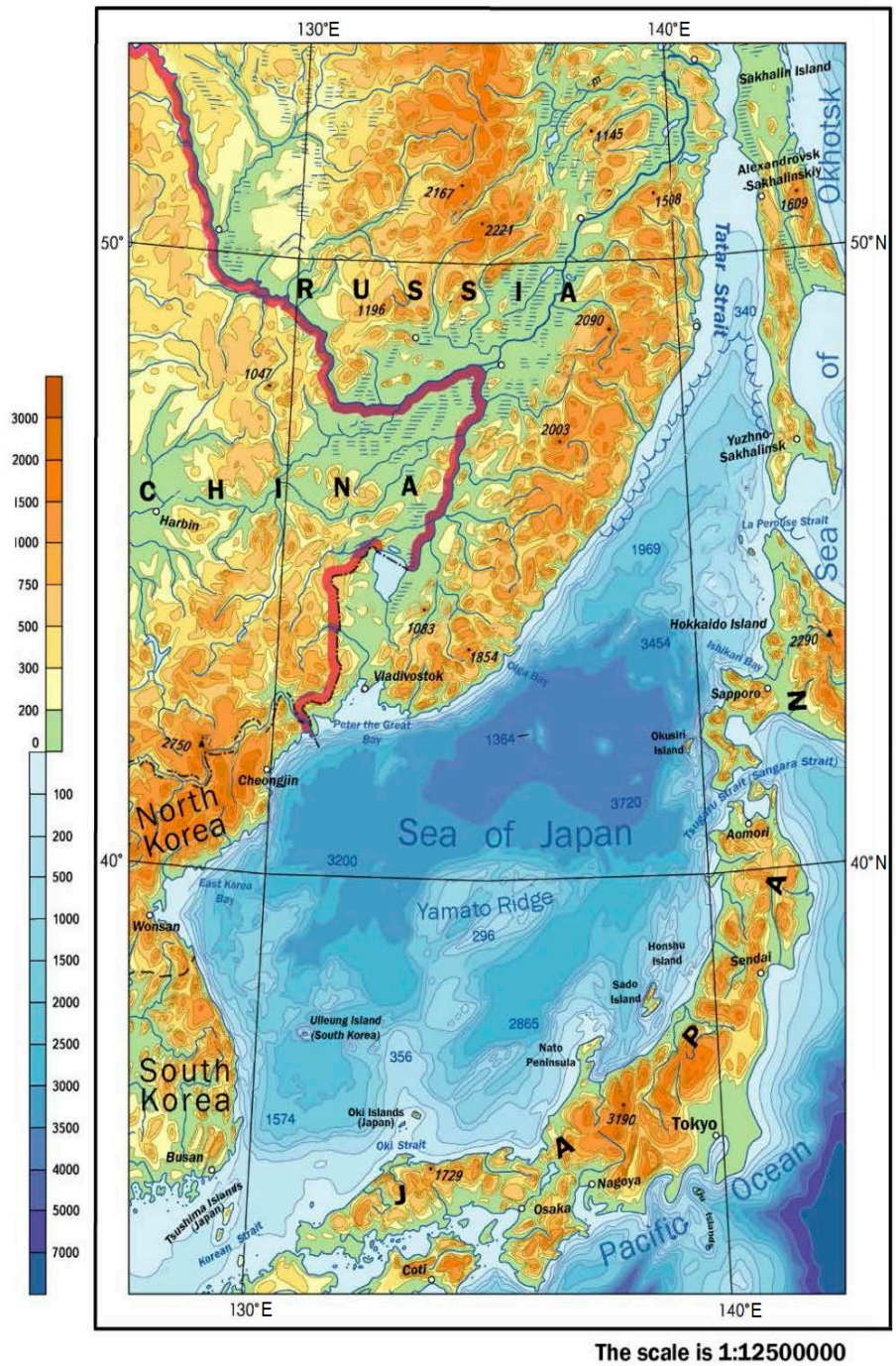

F i g. 1. Physical map of the Sea of Japan [4]

[4] Kotlyakov, V.M., ed., 2004. *National Atlas of Russia. Vol. 2: Nature. Ecology*. Moscow: FSUE "GOSGISTENTR", 495 p. Available at: https://nationalatlas.ru/tom2/294-296.html [Accessed: 30 August 2023] (in Russian).

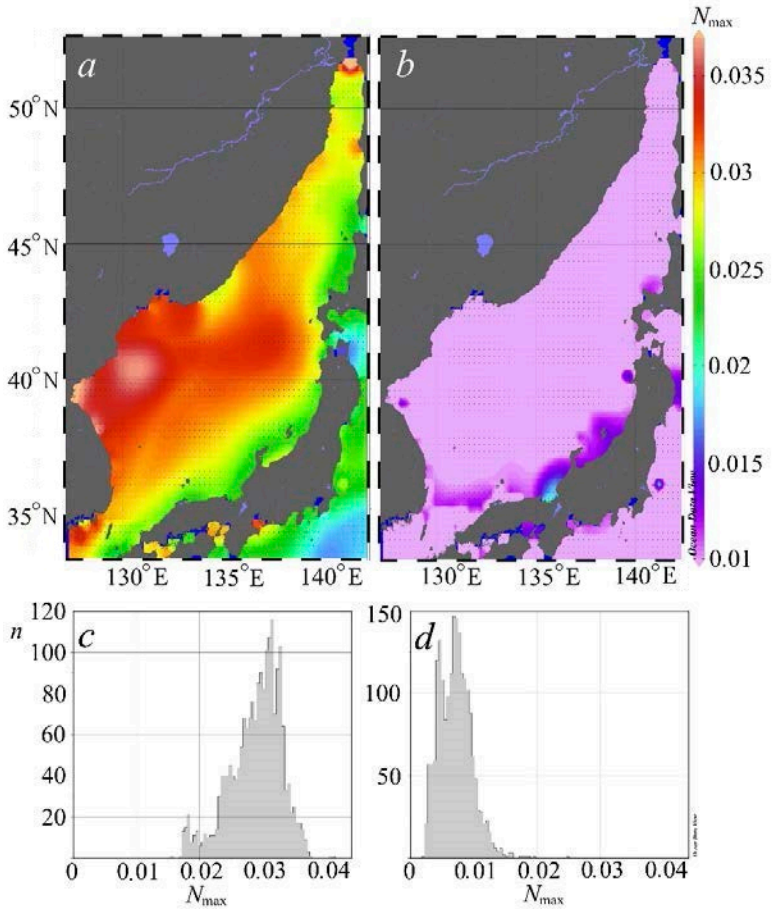

F i g. 2. Spatial distribution of the maximum values of the Brunt – Väisälä frequency (s^{-1}) in the buoyancy profile (*a*, *b*) and histograms of their distribution (*n* is the number of points with the N_{max} values in the selected interval, the entire range of values is divided into 100 intervals, 1957 points in total) (*c*, *d*). Here and below in all the figures, the left panel shows the data for a summer season, the right one – for a winter season

Depths of N_{max} occurrence (Fig. 3) in summer during warming up change mainly in the range of 7–35 m: on the western shelf, the maximum occurrence depth is 15–20 m, gradually shifting to 7–10 m in the coastal zone, and in the southeastern zone it reaches 30–35 m, especially near the southern coast; near the southern coast of the Hokkaido Island, it is 45 m, as there is a deeply heated sea and the main pycnocline is identified.

In winter, the N_{max} horizon map has clearly defined zones of homogeneous depths. This is determined both by bathymetry (the Yamato Plateau is highlighted) and other geographical conditions (river inflows, currents, etc.). In summer, according to Fig. 3, *c*, the distribution of burial depth N_{max} is very narrow (0–35 m), in winter it is very wide. The main depth here is at the sea surface, but comparable maxima in the histogram are reached at depths of 50, 70, and 120 m.

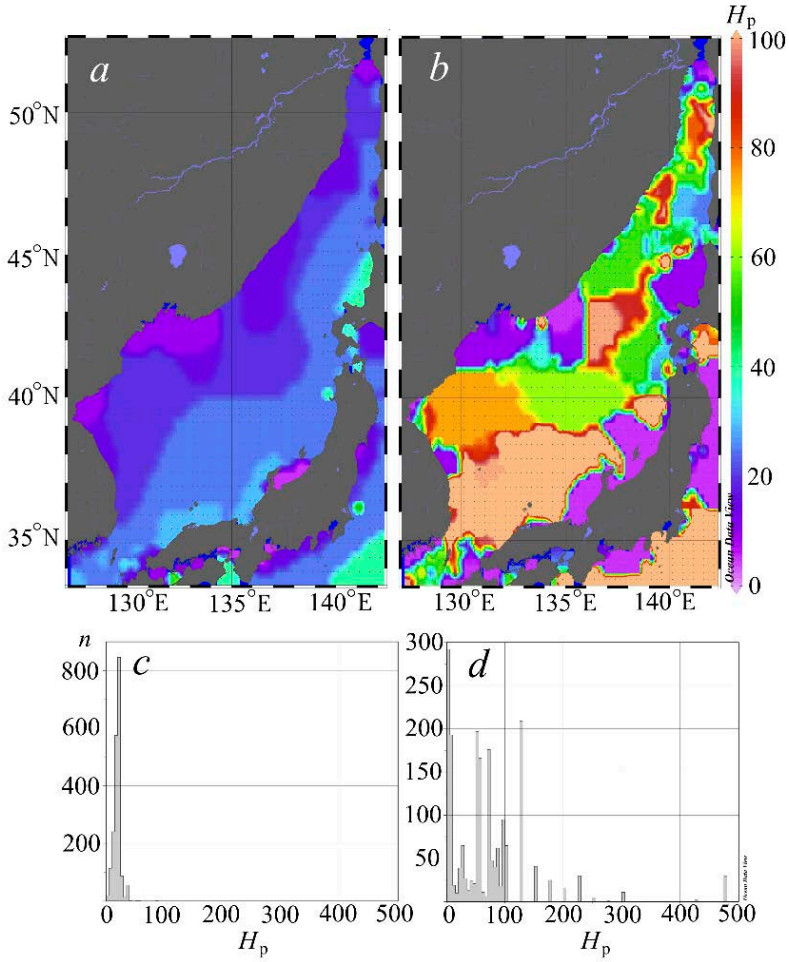

F i g. 3. Maps of the depths (H_p, m) of buoyancy frequency maxima (*a*, *b*), and histograms of their distribution (*c*, *d*)

Theoretical model of solitary internal waves

The internal wave evolution model used in our studies is based on the Gardner equation [17], it was verified using field data (see, e.g., [18]) and describes the propagation of long nonlinear internal waves quite well. Gardner equation is as follows:

$$\frac{\partial \eta}{\partial t} + \left(c + \alpha\eta + \alpha_1\eta^2\right)\frac{\partial \eta}{\partial x} + \beta\frac{\partial^3 \eta}{\partial x^3} = 0, \quad (1)$$

and in a reference frame moving with the long internal wave speed (c),

$$\frac{\partial \eta}{\partial t} + \left(\alpha\eta + \alpha_1\eta^2\right)\frac{\partial \eta}{\partial x} + \beta\frac{\partial^3 \eta}{\partial x^3} = 0. \quad (2)$$

In both equations, η is the isopycnal displacement in the mode function Φ maximum, found from the Sturm–Liouville theory:

$$\frac{d}{dz}\left((c_n - U)^2 \frac{d\Phi_n}{dz}\right) + N^2(z)\Phi_n = 0, \quad \Phi_n(0) = \Phi_n(H) = 0, \quad n = 1, 2, 3,$$

where c_n are the eigenvalues corresponding to the linear velocities of propagation of internal waves of different modes; Φ_n are eigen mode values; $N(z)$ is the Brunt-Väisälä frequency, or buoyancy frequency; $U(z)$ is the shear current velocity. Normalization conditions for the lowest mode: $\Phi_{1max} = \Phi(z_{max}) = 1$ For normalization conditions for the second and higher modes, see [13]). The Gardner equation parameters are found in the mode function quadratures, its derivatives, and the nonlinear correction to it, i.e., they are ultimately determined by the vertical density stratification of the fluid and the current velocity [17]. It should be noted that the dispersion parameter in equations (1), (2) is always positive. However, both nonlinearity parameters can change sign at corresponding depths and stratifications [17].

The one-soliton solution to equation (2) has the following form

$$\eta(x,t) = \frac{A}{1 + B\mathrm{ch}(\gamma(x - Vt))}, \tag{3}$$

$$A = \frac{6\beta\gamma^2}{\alpha}, \qquad B^2 = 1 + \frac{6\alpha_1\beta\gamma^2}{\alpha^2}, \qquad V = \beta\gamma^2,$$

where γ *is* an arbitrary parameter that has the meaning of the inverse width scale. It is also possible to write the parameters of solution (3) A, B, γ in terms of its amplitude a = *A*/(1+*B*):

$$B = a\frac{\alpha_1}{\alpha} + 1, \qquad A = a(a\frac{\alpha_1}{\alpha} + 2), \qquad \gamma^2 = \alpha a(a\frac{\alpha_1}{\alpha} + 2)\frac{1}{6\beta}.$$

It should be noted that within the framework of the Gardner equation with negative cubic nonlinearity, solitons have a polarity that coincides in sign with the quadratic nonlinearity parameter, and are limited in amplitude by the limiting, or thick, soliton amplitude

$$a_{\mathrm{lim}} = -\alpha/\alpha_1. \tag{4}$$

With positive cubic nonlinearity, within the framework of equation (1), solitons of both polarities can exist; only solitons with an amplitude opposite to the quadratic nonlinearity sign cannot have an amplitude less than the algebraic soliton amplitude

$$a_{\mathrm{alg}} = -2\alpha/\alpha_1. \tag{5}$$

Possible branches of the family of solutions (3) for various combinations of signs of the quadratic nonlinearity parameters of the Gardner equation (2) are shown in Fig. 4.

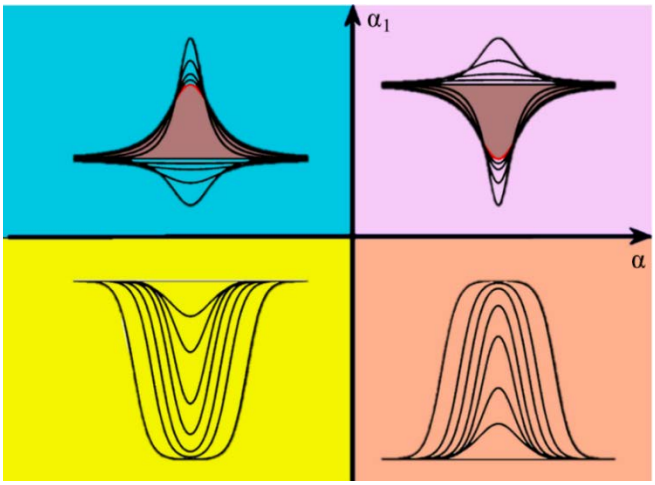

F i g. 4. Possible types of solitons on the plane of the quadratic and cubic nonlinearity (α, α_1) parameters

The characteristics of the mentioned types of localized waves depend on the Gardner equation parameters and, ultimately, on the stratification. Therefore, it is important to know the geographic distribution of the evolutionary model parameters in the considered water areas to understand what type of waves can exist in one or another part of the sea. For this purpose, maps of internal wave parameters are synthesized.

Atlas of kinematic parameters of internal waves (model parameters)

This atlas includes a map of propagation speed of long linear internal waves - *c*, a map of quadratic α and cubic α_1 nonlinearity parameters, a map of dispersion parameter β. Based on the aforementioned maps, the possible forms of internal solitons in the Sea of Japan were studied.

The maps of model parameters are given below only for the lowest, i. e. main, mode. Maps of linear parameters for internal waves – *c* and β – are presented in Figs. 5, *a*, *b* and 6, *a*, *b* respectively. Their seasonal changes here are quite contrasting, the speed and dispersion of waves in summer are everywhere higher than in winter, although the main features of their geographical distribution do not change from season to season. These parameters in the World Ocean are determined mainly by bathymetry, but this is not the case for the Sea of Japan. The main depth exceeding 3 km here lies in a basin in the northern part, and the maximum values of linear parameters are reached in the southern part, in the more pronounced stratification area. In summer, in the northwestern part, the speed of internal waves does not exceed 0.8 m· s^{-1}, and in the southeastern part it is twice as high and reaches 1.6 m· s^{-1}; in winter, in the northwestern part, the speed varies in the range of 0.2–0.4 m· s^{-1}, while in the southeast the maximum speed is still high and reaches 1.3 m· s^{-1}. Histograms of the propagation speed of long internal waves are shown in Fig. 5, *c*, *d*. Although the speed range is the same in summer and winter, the peak of the most frequently occurring values corresponds to a speed of 0.85 m· s^{-1} in summer and 0.2 and 0.5 m· s^{-1} (two peaks) in winter.

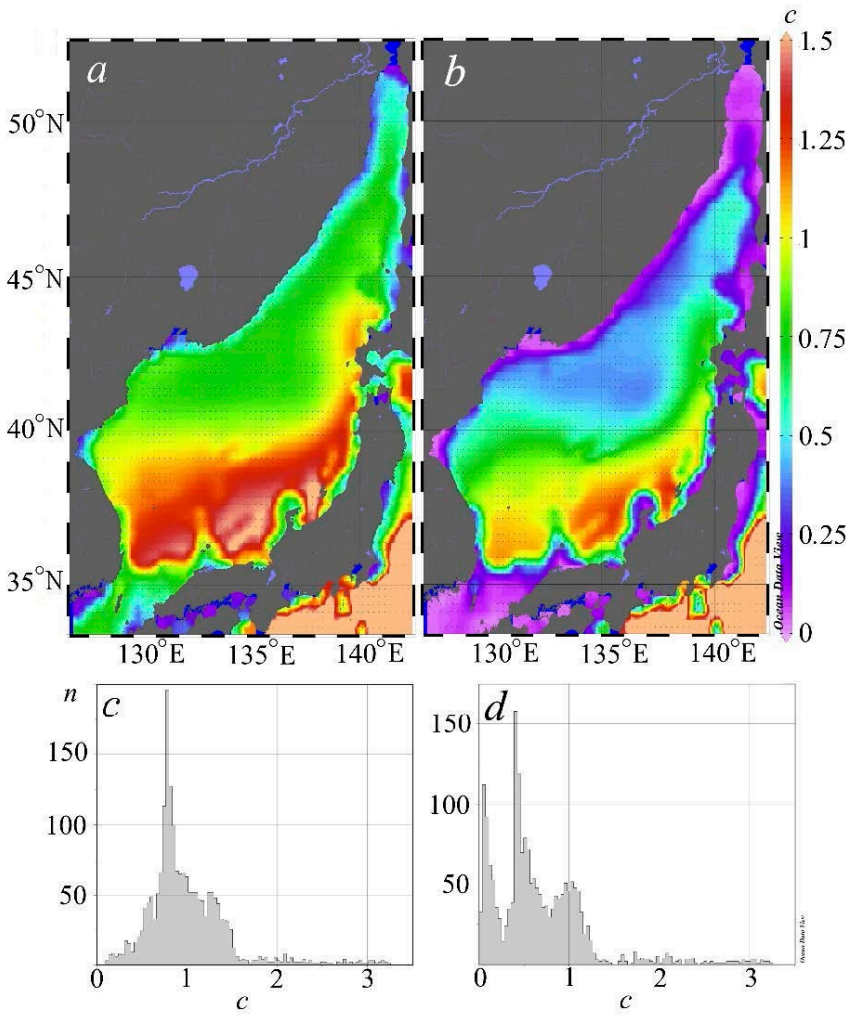

F i g. 5. Maps of the propagation speeds (c, m· s^{-1}) for long linear internal waves of the lowest mode (*a*, *b*), and histograms of their distribution (*c*, *d*)

Fig. 7, *a*, *b* shows the phase velocity correlation with sea depth in summer and winter, respectively. Here, two branches of velocity parameters are clearly distinguished, the branch of lower values corresponds to points in the Sea of Japan, and the upper branch corresponds to a few points of the Pacific Ocean, which, when cutting data from the atlas over a rectangular area, involuntarily end up in processing.

Fig. 7 shows convincingly that there is no dependence of propagation speed for long internal waves on depths over 200 m for the Sea of Japan, although such a dependence can be observed with a small scatter for the Pacific Ocean branch. Also, c values in the Sea of Japan in winter are characterized by a direct correlation with the maximum of the Brunt-Väisälä frequency, although no such dependence is observed for summer season.

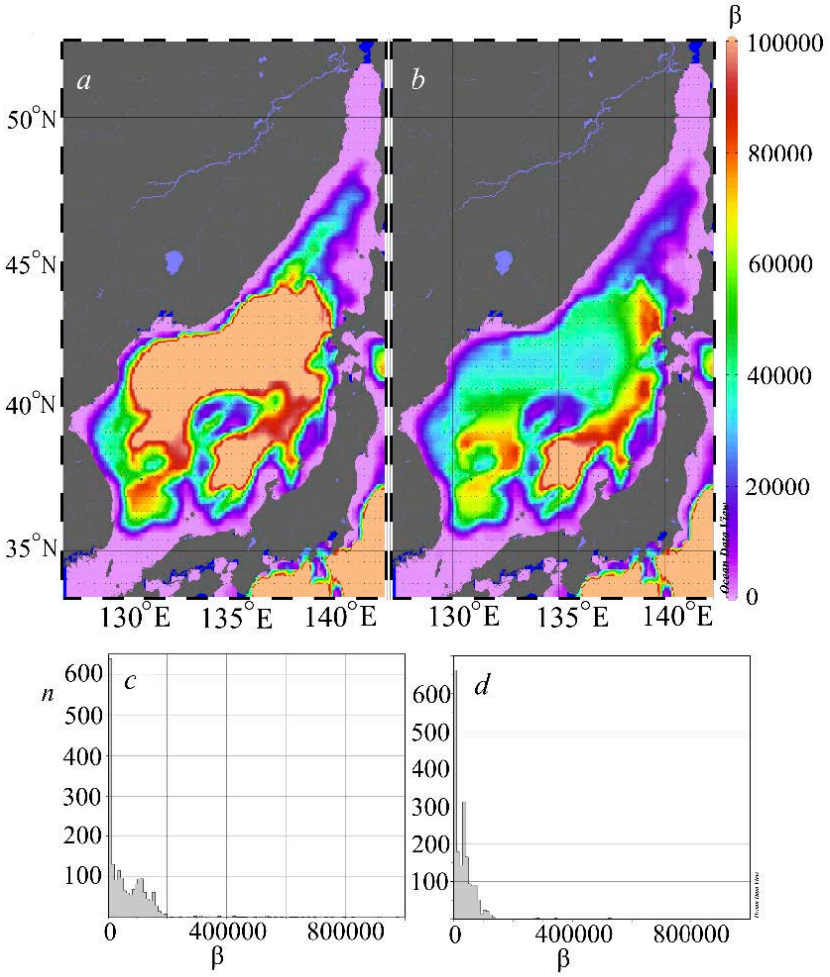

F i g. 6. Values of the dispersion parameter (β, $m^3 \cdot s^{-1}$) of long linear internal waves of the lowest mode (*a*, *b*), and histograms of their distribution (*c*, *d*)

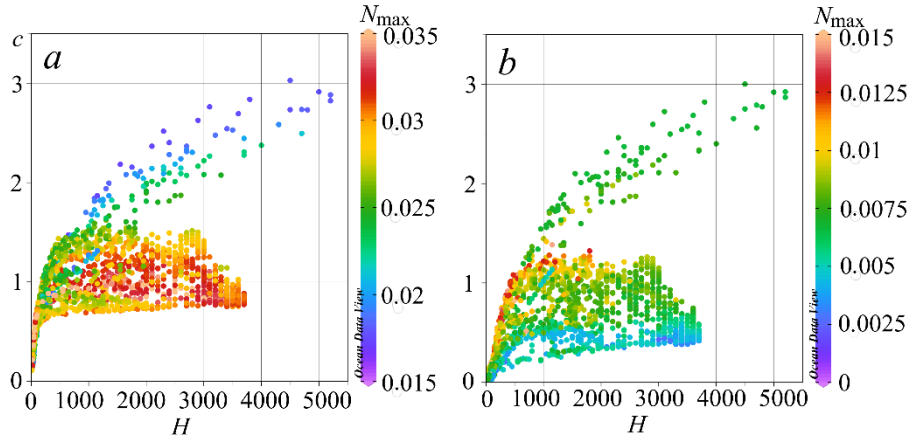

F i g. 7. Propagation speed of long linear internal waves (*c*, $m \cdot s^{-1}$) depending on the sea total depth (*H*, m)

The dispersion parameter (Fig. 6) in the central and southern Sea of Japan also strongly depends on the season. Its maximum value in summer and winter is ~ 105 $m^3 \cdot s^{-1}$, but in summer these values occupy a much larger area.

For the dispersion parameter, the relationship with sea depth is slightly more pronounced than for wave propagation speed, especially in winter. This is clearly visible in Fig. 8, *a*, *b* (lower point cloud) for summer and winter seasons, correspondingly. The upper branch in two fragments corresponds to the Pacific Ocean data. For winter season in 1000–2500 m depth zones, the dependence of the dispersion parameter values on N_{max} stands out clearly. In Fig. 6, *a*, *b*, in winter and summer, the Yamato Rise is clearly marked. In the northern part of the sea (southern part of the Tatar Strait), the dispersion parameter changes slightly from summer to winter, the same topology and almost the same values remain, ~ 5·103 $m^3 \cdot s^{-1}$. In winter, the zone near the Okushiri Island stands out with a high value of the dispersion parameter, where the basin is located; in summer, the dispersion parameter values are higher than in winter, but they are approximately the same around the Yamato Plateau in the central part of the sea. The basin zone is not identified in summer. Nevertheless, on average, the dispersion parameter values are higher in the southern part of the sea than in the central and northern parts.

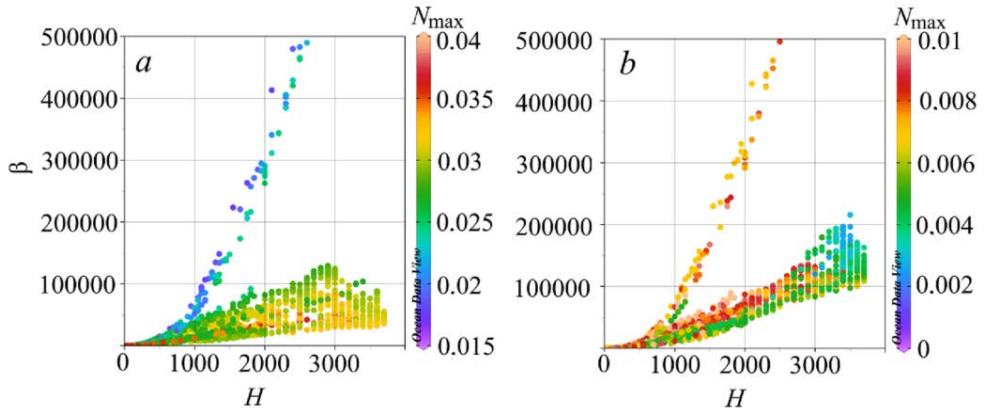

F i g. 8. Dispersion parameter (β) depending on the sea total depth (*H*, m)

Maps of the quadratic nonlinearity parameter (α) are shown in Fig. 9. This parameter is very sensitive to the season, i.e. to the water stratification. From the histograms of values α, it can be seen that in summer this parameter is mainly negative and reaches values in the range of – 0.03 ... 0.01 s^{-1}. However, there are positive parameter areas near the coast, although they are quite few. They are located near the Hokkaido Island, the coast of North Korea and the Gamov Peninsula.

As a result of warming of the upper layers of water and the fresh water flow (due to melting waters in the Sea of Okhotsk), a noticeable seasonal summer pycnocline occurs in the Sea of Japan. Closer to winter, when both heating and fresh water flow stop, this pycnocline is weakly expressed. Then the main role in the formation of the quadratic nonlinearity parameter sign is played by the main

pycnocline position, which is pressed to the bottom, especially in the shelf zone, since water is saltier there. Therefore, in winter, the quadratic nonlinearity parameter changes sign over a noticeable sea area. The histograms in Fig. 9, *c*, *d*, show a significant spread of the quadratic nonlinearity parameter in summer from –0.03 to 0.01 s^{-1} with wide maxima ~ –0.017 and –0.025 s^{-1}. In winter, the range is much smaller, from 0.01 to 0.01 s^{-1} with a narrow high maximum at –0.001 s^{-1}.

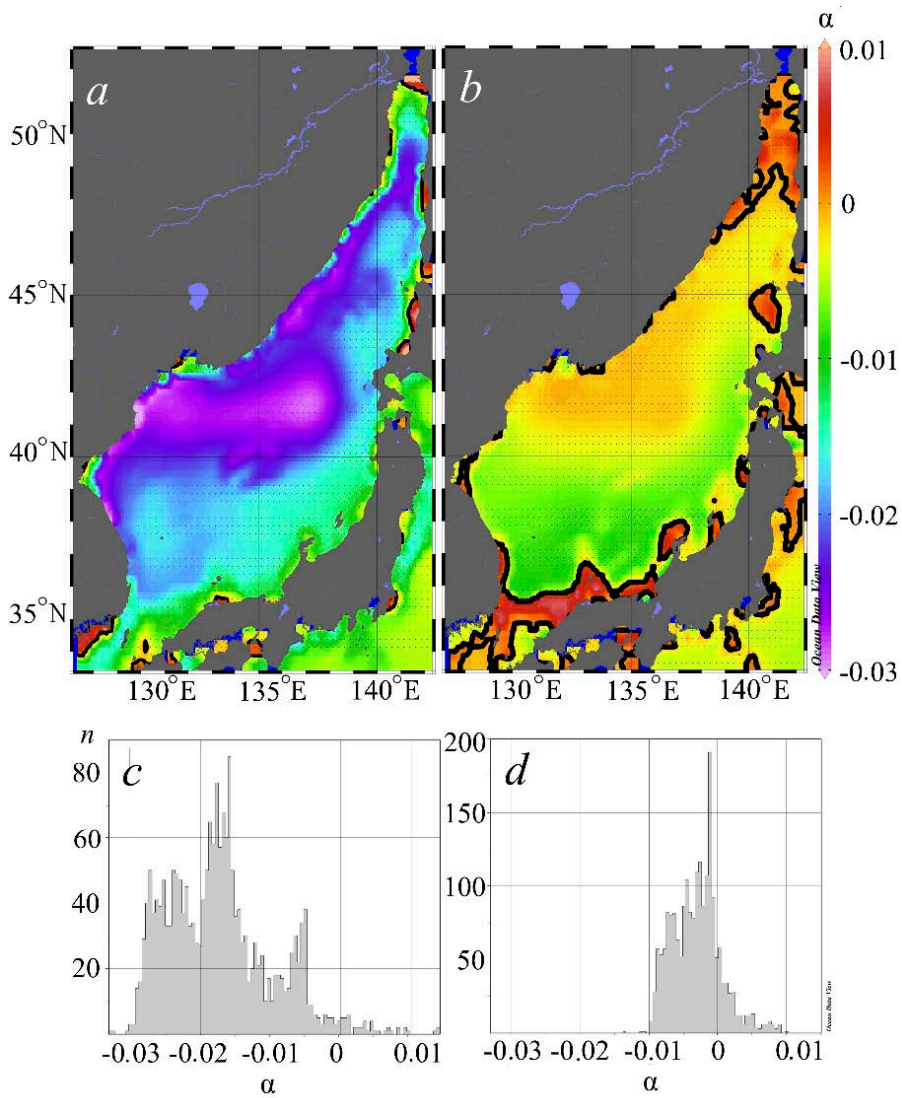

F i g. 9. Maps of the quadratic nonlinearity parameter values (α, s^{-1}) (the black thick line shows the contour of sign change) (*a*, *b*), and histograms of their distribution (*c*, *d*)

Seasonal maps of the cubic nonlinearity parameter are shown in Fig. 10. It should be noted that in summer, a noticeable positive cubic nonlinearity prevails over almost the entire area of the Sea of Japan, which is clearly seen from the summer histogram. As already assumed, in summer the same two main

factors play a role in the stratification formation – warming up the water and the fresh water inflow over the surface due to the ice melting in the Sea of Okhotsk, creating two pycnoclines, and the lower one, consisting of salt water, can be washed out. Although the positive cubic nonlinearity parameter in summer is small (0–0.0005 $(m \cdot s)^{-1}$, individual emissions are up to 0.0017 $(m \cdot s)^{-1}$, it can also change the dynamics of internal waves significantly in the northern part of the Sea of Japan near the Russian coast, in particular, near Cape Gamov. The winter histogram demonstrates a very small, almost zero, cubic nonlinearity parameter of both signs, with negative values predominating. Black thick lines in Fig. 10, *a*, *b* also show the sign change boundary of the cubic nonlinearity parameter. Histograms of the cubic nonlinearity parameter (Fig. 10, *c*, *d*) show its fairly wide distribution over the Sea of Japan in the range – 0.0025 ... 0.001 $(m \cdot s)^{-1}$ with one peak at the point 0.0001 $(m \cdot s)^{-1}$ and a neighbouring peak at the point 0.0005 $(m \cdot s)^{-1}$ in the summer season and a very narrow distribution in the range – 0.0001 ... 0.0001 $(m \cdot s)^{-1}$ with a peak near zero in winter.

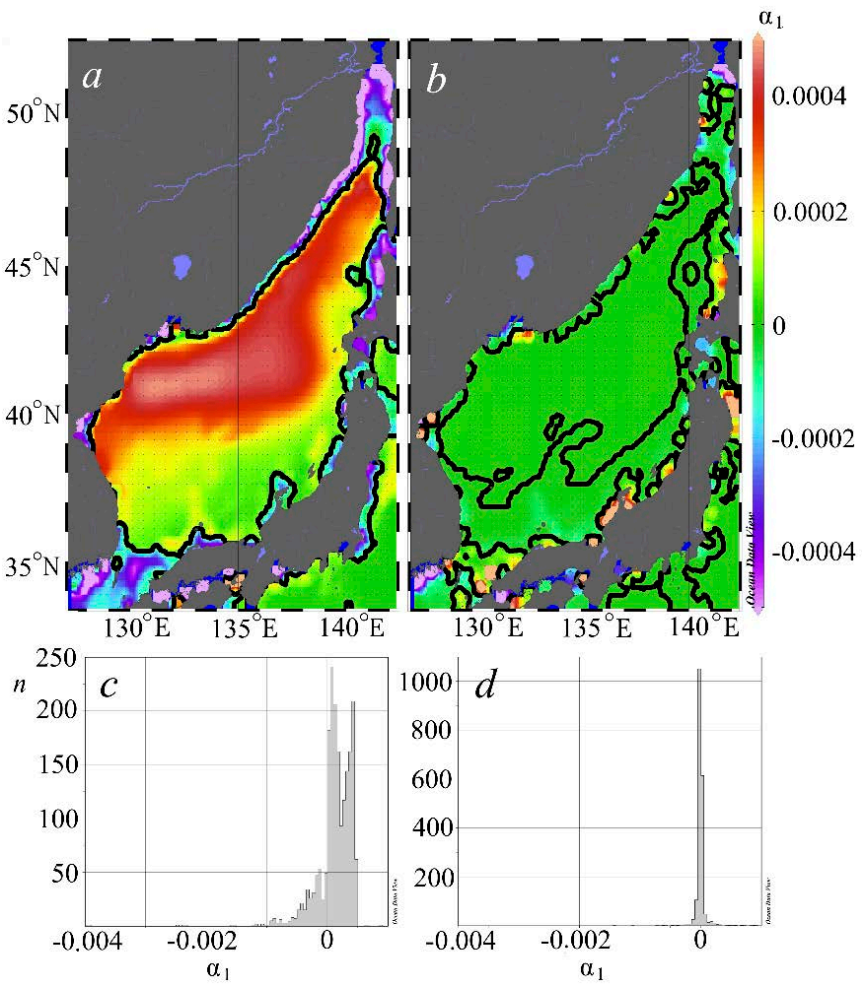

F i g. 10. Maps of the cubic nonlinearity parameter values (α_1, $(m \cdot s)^{-1}$) (*a*, *b*), and histograms of their distribution (*c*, *d*)

Using the Gardner equation parmeters (1), it is possible to determine the branches and limiting amplitudes of possible solitary soliton-like internal waves that can appear in the Sea of Japan. Gardner's classification of solitons is shown in Fig. 4. As already mentioned, if the cubic nonlinearity parameter α_1 in equation (1) is negative, then the solitons in absolute value are limited from above by the amplitude modulus (formula (4)) of a thick, or table-shaped, soliton (Fig. 4, lower half-plane). If the cubic nonlinearity parameter is positive (Fig. 4, upper half-plane), then solitons having opposite polarity to the sign of the quadratic nonlinearity parameter α are limited in absolute value from below by the amplitude modulus (formula (5)) of the algebraic soliton.

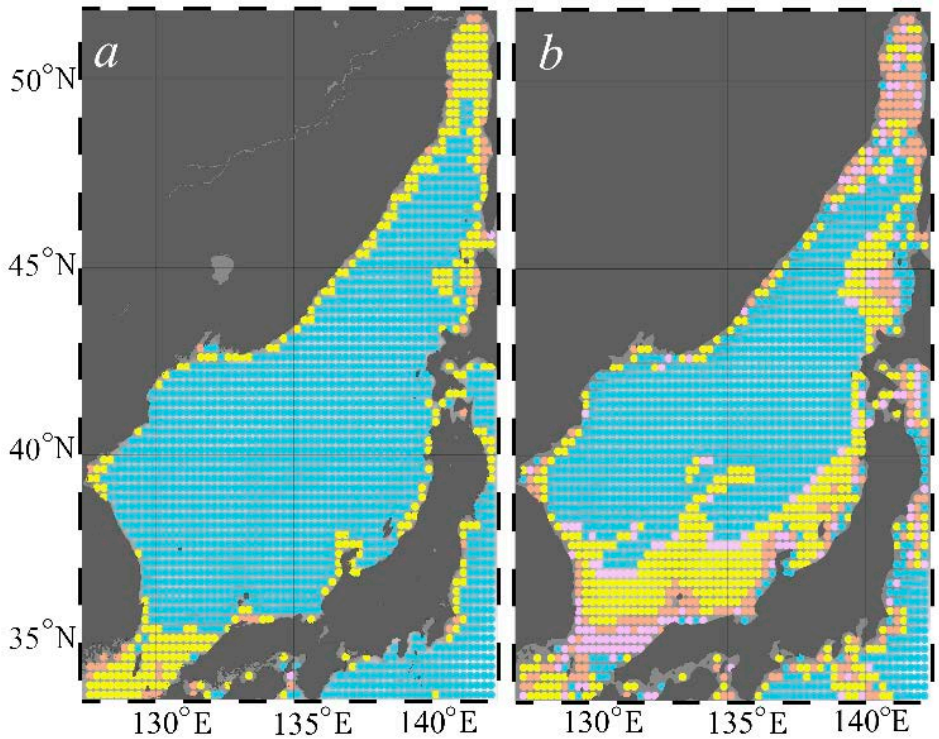

F i g. 11. Distribution of possible soliton types (marked in the same colors as in Fig. 4) in summer (*a*) and in winter (*b*)

Fig. 11 shows that in both winter and summer the main part of the sea is dominated by solitons from the second (blue) quadrant, i.e., the Gardner equation solitons with positive cubic and negative quadratic nonlinearity parameters. In fact, since the cubic nonlinearity parameter in the central part of the sea is quite small, especially in winter, these should be practically solitons of the Korteweg-De Vries equation of negative polarity. Solitons of positive polarity (with an amplitude greater than the amplitude of an algebraic soliton) are possible here only with an amplitude greater than 15–20 m in summer, which, of course, is quite feasible, and ~ 200 m in winter, which goes beyond the weakly nonlinear theory applicability for the Sea of Japan.

Fig. 12 illustrates the nature of the distribution of limiting amplitudes for a thick soliton a_{lim} (formula (4)), for negative values of cubic nonlinearity parameter α_1. For the conditions of the Sea of Japan, the calculated values of the limiting amplitudes – a_{lim} (formula (4)) and a_{alg} (formula (5)) – turn out to be huge in magnitude at the vast majority of points, indicating the impossibility of these restrictions, and with positive cubic nonlinearity – the impracticability of the branch solutions with algebraic soliton. Real amplitudes for a thick soliton seem to be amplitudes of < 100 m (but not exceeding the physical height of the entire water column, i.e., the total depth of the sea). Thick solitons of both polarities with such amplitudes can theoretically appear in the southern part of the Tatar Strait and in coastal zones, as well as in the strait between the coast of South Korea and the Honshu Island. In both winter and summer, such solitons are possible only in coastal zones, and in winter there are more points where this restriction applies than in summer, and the limiting amplitudes of a wide soliton in winter turn out to be greater than in summer.

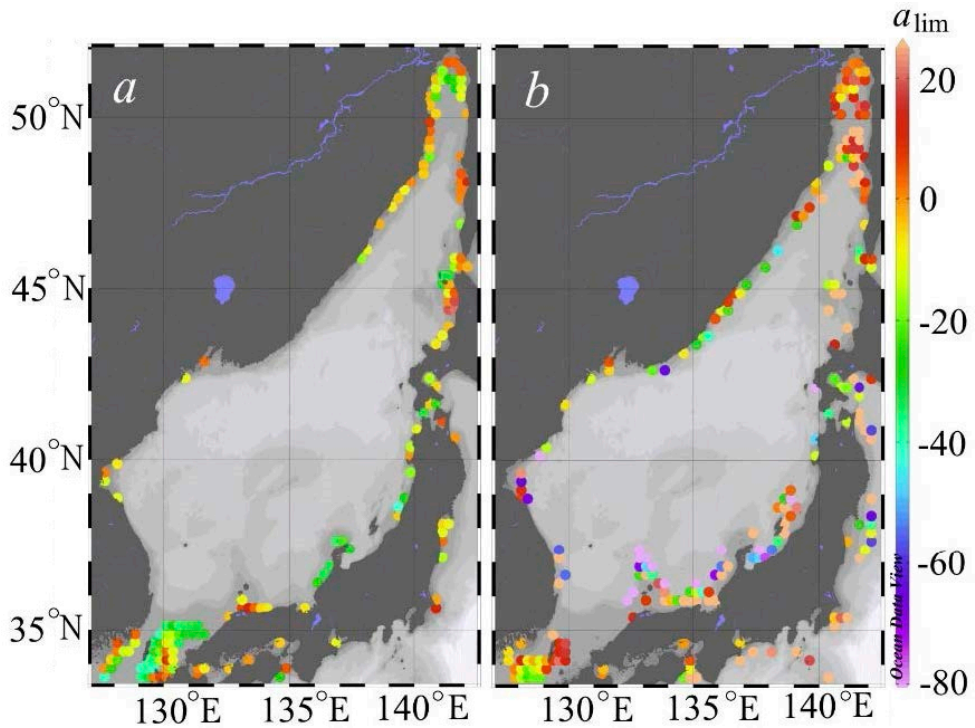

F i g. 12. Maps of the limiting amplitude ($a_{lim} = -\alpha/\alpha_1$ (m)) values for a thick soliton in summer (*a*) and in winter (*b*)

Conclusion

Based on the available data from the international hydrological atlas WOA18, the water density stratification features, kinematic parameters, and limiting amplitudes of internal waves for the Sea of Japan were calculated and presented in the form of an atlas of geographic maps. It is shown that the Brunt-Väisälä frequency maximum and the depth of its occurrence depend on the season

significantly. These parameters, in turn, give an idea of the severity of the internal waves dynamics. The strongest vertical stratification of water density in the Sea of Japan is expectedly observed in summer and autumn. Accordingly, the kinematic parameters for internal waves are most significant in the summer-autumn period. It is shown that such linear parameters as the propagation speed for long internal waves and the dispersion parameter, for which in the World Ocean there is a strong dependence on bathymetry in the Sea of Japan, have a significant range of values at the same depths and are more season-dependent. Based on the calculated parameters, maps of the localized internal wave types possible in the Sea of Japan and the limiting amplitudes of various families of solitons were also constructed.

It should be noted that the model used is capable of adequately describing the behavior of internal waves in coastal waters under the condition of a smooth (compared to the scale of the long-wave processes under consideration) change in the environment properties both in space and in time. However, in the shelf zone of the Sea of Japan to depths of ~ 40 m in summer-autumn period, changes in the thermostratification structure are possible several times a day under the effect of factors external to internal waves (for example, seiche oscillations, passage of eddy structures, etc.) – from practically homogeneous to developed linear stratification. Therefore, for the successful application of a Gardner equation-based model in such conditions and areas, more detailed hydrology is required: the model can quite accurately reproduce internal wave fields qualitatively and quantitatively if the parameters are recalculated according to the current stratification, which has been carried out repeatedly for various World Ocean regions.

REFERENCES

1. Garwood, J.C., Musgrave, R.C. and Lucas, A.J., 2020. Life in Internal Waves. *Oceanography*, 33(3), pp. 38-49. doi:10.5670/oceanog.2020.313
2. Wang, T., Huang, X., Zhao, W., Zheng, S., Yang, Y. and Tian, J., 2022. Internal Solitary Wave Activities near the Indonesian Submarine Wreck Site Inferred from Satellite Images. *Journal of Marine Science and Engineering*, 10(2), 197. doi:10.3390/jmse10020197
3. Li, J., Zhang, Q. and Chen, T., 2021. Numerical Investigation of Internal Solitary Wave Forces on Submarines in Continuously Stratified Fluids. *Journal of Marine Science and Engineering*, 9(12), 1374. doi:10.3390/jmse9121374
4. Chen, M., Chen, K., You, Y.-X. and Yu, H.-T., 2018. Experimental Study of Forces on a Multi-Column Floating Platform in Internal Solitary Waves. *Applied Ocean Research*, 78, pp. 192-200. doi:10.1016/j.apor.2018.06.014
5. Chin-Bing, S.A., Warn-Varnas, A., King, D.B., Hawkins, J. and Lamb, K., 2009. Effects on Acoustics Caused by Ocean Solitons, Part B: Acoustics. *Nonlinear Analysis: Theory, Methods & Applications*, 71(12), pp. e2194-e2204. doi:10.1016/j.na.2009.04.069
6. Duda, T.F., Lynch, J.F., Irish, J.D., Beardsley, R.C., Ramp, S.R., Chiu, C.-S., Tang, T.Y. and Yang, Y.-J., 2004. Internal Tide and Nonlinear Internal Wave Behavior at the Continental Slope in the Northern South China Sea. *IEEE Journal of Oceanic Engineering*, 29(4), pp. 1105-1130. doi:10.1109/JOE.2004.836998
7. Shroyer, E.L., Moum, J.N. and Nash, J.D., 2010. Mode 2 Waves on the Continental Shelf: Ephemeral Components of the Nonlinear Internal Wavefield. *Journal of Geophysical Research: Oceans*, 115(C7), C07001. doi:10.1029/2009JC005605
8. Talipova, T., Kurkina, O., Kurkin, A., Didenkulova, E. and Pelinovsky, E., 2020. Internal Wave Breathers in the Slightly Stratified Fluid. *Microgravity Science and Technology*, 32(1), pp. 69-77. doi:10.1007/s12217-019-09738-2

9. Dolgikh, G.I., Novotryasov, V.V., Yaroshchuk, I.O. and Permyakov, M.S., 2018. Intense Undular Bores on the Autumn Pycnocline of Shelf Waters of the Peter the Great Bay (Sea of Japan). *Doklady Earth Sciences*, 479(1), pp. 379-383. doi:10.1134/S1028334X18030157

10. Lee, J.H., Lozovatsky, I., Jang, S.-T., Jang, Ch.J., Hong, C.S. and Fernando, H.J.S., 2006. Episodes of Nonlinear Internal Waves in the Northern East China Sea. *Geophysical Research Letters*, 33(18), L18601. doi:10.1029/2006GL027136

11. Kurkina, O., Pelinovsky, E., Talipova, T. and Soomere, T., 2011. Mapping the Internal Wave Field in the Baltic Sea in the Context of Sediment Transport in Shallow Water. *Journal of Coastal Research*, SI 64, pp. 2042-2047.

12. Kurkina, O., Rouvinskaya, E., Talipova, T. and Soomere, T., 2017. Propagation Regimes and Populations of Internal Waves in the Mediterranean Sea Basin. *Estuarine, Coastal and Shelf Science*, 185, pp. 44-54. doi:10.1016/j.ecss.2016.12.003

13. Kurkina, O., Talipova, T., Soomere, T., Giniyatullin, A. and Kurkin, A., 2017. Kinematic Parameters of Internal Waves of the Second Mode in the South China Sea. *Nonlinear Processes in Geophysics*, 24(4), pp. 645-660. doi:10.5194/npg-24-645-2017

14. Kurkina, O.E., Talipova, T.G., Soomere, T., Kurkin, A.A. and Rybin, A.V., 2017. The Impact of Seasonal Changes in Stratification on the Dynamics of Internal Waves in the Sea of Okhotsk. *Estonian Journal of Earth Sciences*, 66(4), pp. 238-255. doi:10.3176/earth.2017.20

15. Filatov, N.N., 2019. The Modern State and Perspective Investigations of Hydrophysical Processes and Ecosystems of Inland Waters (a Review). *Fundamentalnaya i Prikladnaya Gidrofizika*, 12(1), pp. 3-14. doi:10.7868/S2073667319010015 (in Russian).

16. Lavrova, O.Yu., Mityagina, M.I. and Sabinin K.D., 2011. Study of Internal Wave Generation and Propagation Features in Non-Tidal Seas Based on Satellite Synthetic Aperture Radar Data. *Doklady Earth Sciences*, 436(1), pp. 165-169. doi:10.1134/S1028334X11010272

17. Grimshaw, R., Pelinovsky, E., Talipova, T. and Kurkin, A., 2004. Simulation of the Transformation of Internal Solitary Waves on Oceanic Shelves. *Journal of Physical Oceanography*, 34(12), pp. 2774-2791. doi:10.1175/JPO2652.1

18. Zhang, W., Didenkulova, I., Kurkina, O., Cui, Y., Haberkern, J., Aepfler, R., Santos, A.I., Zhang, H. and Hanebuth, T.J.J., 2019. Internal Solitary Waves Control Offshore Extension of Mud Depocenters on the NW Iberian Shelf. *Marine Geology*, 409, pp. 15-30. doi:10.1016/j.margeo.2018.12.008

About the authors:

Maria V. Kokoulina, Assistant, Nizhny Novgorod State Technical University n.a. R. E. Alekseev (24 Minin Str., Nizhny Novgorod, 603950, Russian Federation); Senior Engineer, V.I. Il'ichev Pacific Oceanological Institute, Far Eastern Branch of the Russian Academy of Sciences (34 Baltiyskaya Str., Vladivostok, 690041, Russian Federation), **ORCID ID: 0000-0001-5890-3649**, **ResearcherID: AAD-7131-2019**, **Scopus Author ID: 57212345658**, **SPIN-code: 3788-0620 AuthorID: 990977**, kokoulinamaria97@gmail.com

Oksana E. Kurkina, Leading Researcher, Nizhny Novgorod State Technical University n.a. R. E. Alekseev (24 Minin Str., Nizhny Novgorod, 603950, Russian Federation), Ph.D. (Phys.-Math.), Associate Professor, **ORCID ID: 0000-0002-4030-2906, ResearcherID G-9577-2011**, Oksana.Kurkina@mail.ru

Tatiana G. Talipova, Leading Researcher, Nizhny Novgorod State Technical University n.a. R. E. Alekseev (24 Minin Str., Nizhny Novgorod, 603950, Russian Federation); Leading Researcher, V.I. Il'ichev Pacific Oceanological Institute, Far Eastern Branch of the Russian Academy of Sciences (34 Baltiyskaya Str., Vladivostok, 690041, Russian Federation), Dr.Sci. (Phys.-Math.), **ORCID ID: 0000-0002-1967-4174**, **ResearcherID: A-1580-2014**, **Scopus Author ID: 7004244713**, **SPIN-code: 4837-6302 AuthorID: 40951**, tgtalipova@mail.ru

Andrey A. Kurkin, Chief Researcher, Head of the Applied Mathematics Department, Scientific Supervisor, Nizhny Novgorod State Technical University n.a. R. E. Alekseev (24 Minin Str., Nizhny Novgorod, 603950, Russian Federation); Leading Researcher, V.I. Il'ichev Pacific Oceanological Institute, Far Eastern Branch of the Russian Academy of Sciences (34 Baltiyskaya Str., Vladivostok, 690041, Russian Federation), Dr.Sci. (Phys.-Math.), Professor, **ORCID ID: 0000-0003-3828-6406**, **ResearcherID: A-1972-2014**, **Scopus Author ID: 7003446660**, **SPIN-code: 1390-3940 AuthorID: 35546**, aakurkin@gmail.com

Efim N. Pelinovsky, Chief Researcher, Nizhny Novgorod State Technical University n.a. R. E. Alekseev (24 Minin Str., Nizhny Novgorod, 603950, Russian Federation); Chief Researcher, V.I. Il'ichev Pacific Oceanological Institute, Far Eastern Branch of the Russian Academy of Sciences (34 Baltiyskaya Str., Vladivostok, 690041, Russian Federation), Dr.Sci. (Phys.-Math.), Professor, **ORCID ID: 0000-0002-5092-0302**, **ResearcherID: I-3670-2013**, **Scopus Author ID: 7004951110**, **SPIN-code: 8949-9088 AuthorID: 103314**, pelinovsky@gmail.com

Contribution of the co-authors:

Maria V. Kokoulina – computer software debugging to solve tasks, preparation of figures, participation in the discussion of paper materials

Oksana E. Kurkina – preparation of the paper text, formulation of paper objectives, qualitative and quantitative analysis of the results

Tatiana G. Talipova – literature selection and analysis

Andrey A. Kurkin – scientific supervision, critical analysis and revision of the text

Efim N. Pelinovsky – data systematization, qualitative analysis of the results

The authors have read and approved the final manuscript.
The authors declare that they have no conflict of interest.